High Stiffness Nano-composite Fibres from Polyvinylalcohol filled with Graphene and Boron Nitride

Conor S Boland, Sebastian Barwich, Umar Khan and Jonathan N Coleman*[1]

School of Physics, CRANN and AMBER, Trinity College Dublin, Dublin 2, Ireland

ABSTRACT: Here we describe using nanosheets of both graphene and boron nitride, produced by liquid phase exfoliation, as fillers in composite fibres. The fibres were prepared by coagulation spinning using polyvinylalcohol as a matrix. We obtained good quality fibres with diameter and nanosheet volume fraction which could be controlled via the ratio of nanosheet to polymer injection rates. The mechanical stiffness (modulus, Y) and strength, σ_B, increased relatively slowly with volume fraction ($dY/dV_f \leq 160$ GPa and $d\sigma_B/dV_f \leq 0.8$ GPa). However, both stiffness and strength continued increasing with nanosheet content to loading levels of ~20vol%, after which the properties fell off. Such relatively high loading levels result in impressive mechanical properties with stiffness and strength of up to 30 GPa and 260 MPa observed. In addition, we found the graphene-filled fibres to be electrically conducting with conductivities of up to 3 S/m.

1. Introduction

Over the last decade, graphene has received unparalleled attention due to its extensive array of superlative physical properties.[1-5] Of particular interest are its mechanical properties. Graphene is both the strongest and stiffest material known, displaying tensile strength and elastic modulus values of σ_B=130 GPa and Y=1000 GPa respectively.[6] As such, it is of great interest to researchers as a filler for reinforcing[7] composites. According to the rule of mixtures, the strength and modulus of reinforced composites are given by[8, 9]

$$Y \approx \eta_0 \eta_{L,Y} Y_{NT} V_f + Y_P \quad (1)$$

$$\sigma_B \approx \eta_0 \eta_{L,\sigma} \sigma_{NT} V_f + \sigma_P \quad (2)$$

[1] Corresponding Author. E-mail: colemaj@tcd.ie, +35318963859 (J.N. Coleman)

where V_f is the graphene volume fraction, Y_{NT} and Y_P are the graphene and polymer moduli respectively while σ_{NT} and σ_P are the graphene and polymer strengths respectively. The appropriate efficiency factors describe the dependence of reinforcement on nanosheet orientation (η_o) and length ($\eta_{L,Y}$ and $\eta_{L,\sigma}$).[8, 9] We note that the length efficiency factors for strength ($\eta_{L,\sigma}$) has two forms,[8, 10] for nanosheets which are longer or shorter than the critical length[7] respectively. In the ideal case where the matrix-graphene interface is well bonded, the nanosheets are well-dispersed and both long and well aligned, the efficiency factors approach their limiting values: $\eta_L \sim \eta_o \sim 1$. Then both modulus and strength increase rapidly with volume fraction. In the best possible scenario $dY/dV_f \approx Y_{NT}$ ~1000 GPa and $d\sigma_B/dV_f \approx \sigma_{NT}$ ~130 GPa. Ideally, these mechanical property increases would continue to reasonably large volume fractions resulting in large absolute strength and stiffness increases. Unfortunately, this never occurs in reality.

In practise,[11] the matrix-graphene interface is well bonded only in certain polymers and only at low-strain,[12] alignment is not guaranteed[13] and the nanosheets are never long enough to get large strength reinforcement. This last point is especially relevant for liquid-exfoliated nanosheets which are generally less than 1 μm in length and so usually below the so-called critical length.[7, 12] Then, failure tends to be by pull-out rather than nanosheet breakage and $d\sigma/dV_f$ becomes controlled by interfacial strength rather than nanosheet strength.[7, 14] This results in a significant reduction in strength enhancement (although dY/dV_f can reach a reasonable fraction of its theoretical maximum[10]). In addition, if the nanosheets are thicker than ~3 layers, they display an effective modulus which is considerably lower than monolayer graphene.[15] However, possibly the greatest problem with graphene-reinforced composites is that aggregation begins to occur at relatively low volume fractions. Above this point the mechanical properties no longer increase and may actually fall. In most cases the aggregation threshold is between ~0.03 and ~4 vol%.[16-19] This results in composites with moduli which are typically up to ×3 higher than the matrix[11, 19] (N.B. this is true for thermoplastic matrices. From elastomeric matrices, larger relative increases are possible, but from a very low base[11]).

In the past, problems involving aggregation and alignment of nano-fillers have often been solved via the formation of fibres rather than bulk composites. For example polymer-nanotube fibres have been produced through melt processing[20-26], coagulation spinning[27-33] and electrospinning[34-42]. This has allowed volume fractions of up to ~60 vol%, resulting

in moduli and strength as high as Y=80 GPa and σ_B=1.8 GPa.[33, 43] However, compared to nanotubes, relatively little work has been done to investigate the potential of 2D nanosheets as fillers in composite fibres. A number of papers have used chemically modified graphene (graphene oxide, GO) as a filler in composite fibres,[44-53] while other groups have studied graphene-oxide-only fibres.[54-65] However, while GO nanosheets may show good polymer-nanosheet stress transfer, they are not ideal reinforcements as they have impaired mechanical properties due to their high defect content (i.e. GO has a measured nanosheet modulus of ~250 GPa[ref[66]] compared to ~1000 GPa for graphene[6]). We would actually expect pristine (i.e. non-oxidised, defect-free) graphene to have some advantages as a filler due to its superior strength and modulus although the nanosheet size may be too small for effective strength enhancement.[11] Such graphene can now be made by sonication[67-69] or shear mixing[70, 71] of graphite in appropriate liquids. However, only one study has yet described fibres filled with pristine graphene.[72] In fact, we believe pristine nanosheets, not only of graphene but also of other inorganic 2D materials such as boron nitride (BN) may have some advantages as reinforcing fillers in composite fibres. BN, in particular has mechanical properties very similar to graphene.[73]

As observed with carbon nanotubes, fibre formation can result in filler alignment and reduced aggregation (compared to bulk composites) at reasonably high loading levels.[31, 32] If this could be achieved for nanosheet-filled fibres, it could result in aggregation thresholds which are considerably higher than in bulk composites and so improved mechanical properties. In this study we report using coagulation spinning to produce fibres of polyvinylalcohol filled with pristine nanosheets of both graphene and boron nitride. Although the BN-based fibres are relatively poor mechanically, for the graphene-filled fibres we find stiffness values of up to 30 GPa, much higher than is usually found for graphene-based composites. In addition, the graphene-filled fibres are electrically conductive, displaying conductivities of up to 3 S/m.

2. Methods

A sodium cholate (Sigma Aldrich) solution was prepared by dissolving the surfactant powder in deionized water at 10 mg/ml and stirring for 4 hours at 40C. A dispersion of Graphene (Sigma Aldrich) and Boron Nitride (H.C. Starck) in N-Methyl-2-pyrrolidone NMP was prepared by ultrasonic tip-sonication (Sonics Vibra Cell model VCX, 750W, 42 kHz) for 72 h at 45% amplitude.[67, 74] These dispersions were mildly centrifuged at 1500 rpm for 90

min. The resultant supernatant contained graphene and BN nanosheets very similar to those reported in a number of papers.[67, 74] This supernatant was then vacuum filtered to form a film that was redispersed in the surfactant solution at high concentration (30 mg/mL) by ultrasonic tip-sonication for 1 hour followed by bath-sonication (Branson 1510 model 42 kHz) for 3 hours.[68, 69, 75] A solution of polyvinyl alcohol (J. T. Baker, M_w = 77,000–79,000 g/mol, 99–99.8% hydrolysed) was prepared in deionised water at C=50 mg/ml. The solution was refluxed at 150°C for ~3 hr until transparent.

TEM grids were prepared by first diluting the dispersions and then drop-casting them onto holey carbon grids (Cu 400 mesh). Residual solvent was removed from the grids by drying in a vacuum oven. Bright field TEM images were obtained using a Jeol 2100 operating at 200 keV.

To prepare the composite fibres, the surfactant-stabilised nanosheet dispersions (inks) were injected at well-defined flow rates into the centre of a cylindrical glass pipe (inner diameter 5 mm) in which the polyvinyl alcohol solution flowed. The graphene ink flow rates ranged from 0.18-2 ml/min at a constant PVA flow rate of 4.61 ml/min. The BN inks were injected at rates in the ranges 7 - 22 ml/min for a PVA flow rate of 50 ml/min and 1 - 18 ml/min for a PVA rate of 30 ml/min. Contact with the PVA solution caused collapse of the dispersion into a continuous fibre, which then travelled down the pipe and was collected in a stationary water bath. Fibres were cut into long sections (~12 cm) and pipetted into a 30:70 water:methanol bath, being left to rest for ~2 min. The fibres were then cut into smaller sections (~3 cm), removed from the solvent bath and dried at 60 C under vacuum for 48 hr.

Scanning electron microscopy (SEM) was performed using a Zeiss Ultra Plus Field Emission Scanning Electron Microscope. Thermogravimetric analysis (Perkin-Elmer Pyris 1) was used to calculate the filler mass fraction of each composite fibre set. Mechanical testing was performed with a Zwick Z100 tensile tester using a 100 N load cell with a strain rate of 1 mm/min with a constant gauge length of 10 mm. Electrical measurements were performed by painting each end of the graphene fibres with silver paint onto a glass slide. Initially, measurements were made with both 2- and 4-probe mode on a Keithley KE2601 source meter. In all cases both techniques gave a similar resistance, indicating that the contact resistance is very small compared to fibre resistance. Subsequently, all measurements were made using 2 probes.

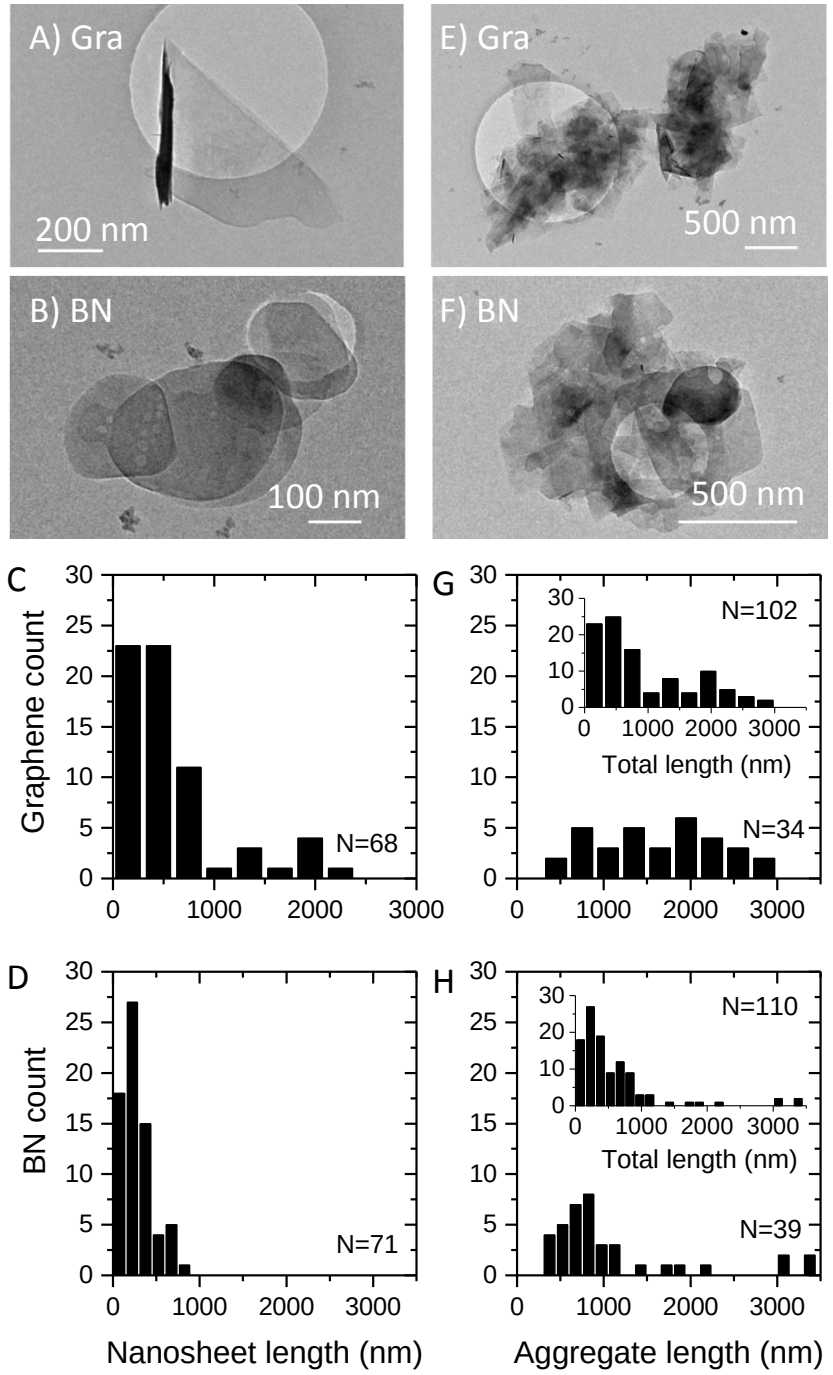

Figure 1: Characterisation of liquid exfoliated graphene and BN nanosheets and aggregates. A-B) TEM images of both graphene (A) and BN (B) nanosheets. C-D) Histograms showing the length of graphene (C) and BN (D) nanosheets. E-F) TEM images of both graphene (E) and BN (F) aggregates. G-H) Histograms showing the length of graphene (G) and BN (H) aggregates. The insets in (G) and (H) show the histograms for nanosheets and aggregates combined.

3. Results and Discussion

3.1 Fibre Formation

In this work we start by preparing dispersions of both graphene and boron nitride nanosheets by liquid phase exfoliation.[67-71, 75] This technique can give dispersions of defect-free nanosheets in surfactant solutions at relatively high concentrations (see methods). The resultant dispersions are ideal for processing into a range of structures,[74, 76] including polymer-nanosheet composites.[10, 14, 72, 77, 78] However, in this work we found that as-produced nanosheets could not be used to prepare composite fibres. We discovered that this could be addressed by using special techniques (see methods) to produce extremely high concentration (~30 mg/mL) dispersions of both graphene and BN nanosheets. However, as such high concentrations may lead to aggregation, it is important to assess the aggregation state of the nanosheets used to prepare the fibres. TEM analysis showed the majority of dispersed objects to be graphene or BN few-layer nanosheets with representative images shown in figure 1 A and B. Shown in figure 1 C-D are histograms showing the lengths of these dispersed nanosheets. We found mean lengths of 580 nm and 280 nm for graphene and BN nanosheets respectively. However, the nanosheets made up only ~2/3 of the objects observed in TEM. The other 1/3 consisted of aggregates of nanosheets as shown in figure 1 E and F. These aggregates were almost certainly formed by flocculation of nanosheets at the extremely high concentrations used in this work. Interestingly, the aggregates were all electron transparent, and so relatively thin, and thus appear to have retained their 2-dimensional nature. Histograms showing the length of graphene and BN aggregates are shown in figure 1 G and H respectively. The mean aggregate lengths were 1660 nm and 1090 nm for Graphene and BN aggregates respectively. Combining nanosheet and aggregate data allows us to generate histograms showing the entire population of 2D objects as shown in the insets of figure 1 G and H. The overall mean lengths extracted from the combined data were 940 nm and 570 nm for graphene and BN respectively.

It is extremely challenging to accurately measure the thickness of liquid exfoliated nanosheets. However, we have previously noted that the mean nanosheet length and thickness (number of monolayers per nanosheet) are roughly related by $\langle L \rangle / \langle N \rangle \sim 60$.[70] Assuming this can be applied here would give a rough estimate of the mean thickness of dispersed 2D objects (nanosheets and aggregates) to be ~16 and 10 for graphene and BN respectively. This translates into actual mean thicknesses of ~5.5 nm and ~3.5 nm respectively

In this work, we used these high concentration dispersions to fabricate polyvinylalcohol (PVA) based composite fibres, filled with graphene and BN nanosheets, using the well-known coagulation-spinning procedure.[30-33, 43] Aqueous dispersions of surfactant stabilized boron nitride (BN) and graphene (G) nanosheets were injected into the centre of a glass pipe through which an aqueous PVA solution was flowing[33]. When exposed to the polymer solution the dispersions destabilize, collapsing to form a continuous fibre. The resultant fibres are then collected in a stationary water bath, after which they were transferred to a methanol bath to increase polymer crystallinity via dehydration.[79] The fibres were then transferred to a vacuum oven to dry.

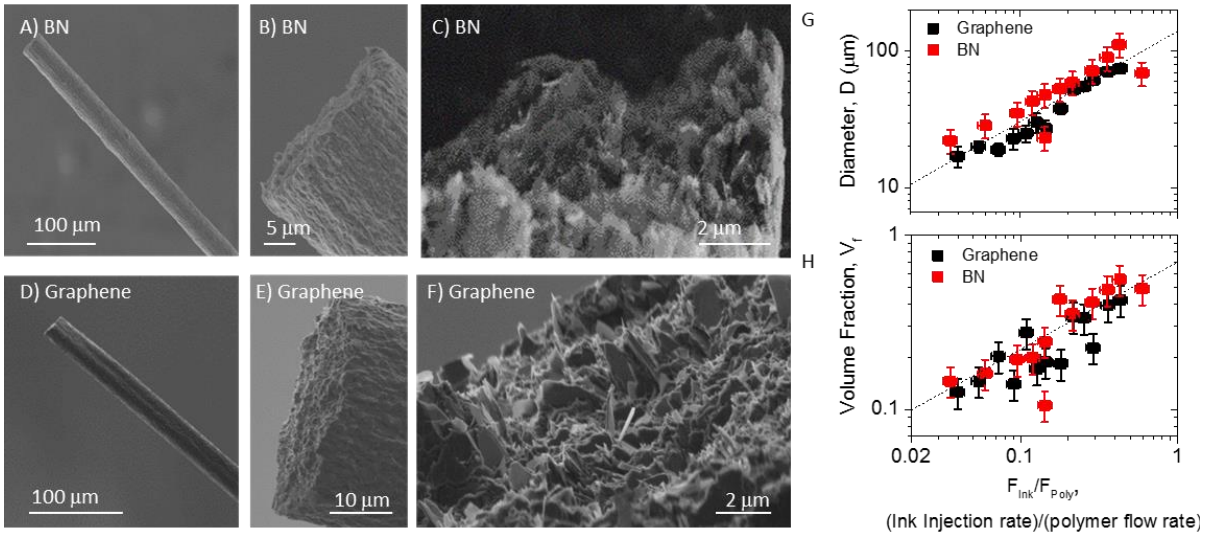

Figure 2. SEM images and formation conditions for graphene and boron nitride composite fibres. (A-F) SEM images of composite (A-C) Boron Nitride and (D-F) Graphene fibres. G-H) Scaling of diameter and volume fraction with the ratio of ink injection rate to polymer flow rate used during fibre preparation. The dashed lines in G and H represent power laws with exponents 0.66 and 0.5 respectively.

Shown in Figure 2A-F are SEM images of the resultant fibres which are generally straight, with an even surface, uniform diameter, and circular cross section. This is in contrast to graphene-only fibres[61, 62, 65, 72, 80, 81], which are usually much less uniform. Close up images of fracture surfaces of both graphene- and BN-filled composite fibres are shown in Figs. 1C and 1F. Here, flakes of filler material can be seen protruding from the surface, suggesting fracture to occur by pull-out.[14, 82] In this mechanism, the nanosheet length is below the critical length and so is too short for stress-transfer from matrix to the filler to result

in nanosheet fracture.[7, 82] As a result, failure occurs at the polymer-nanosheet interface resulting in pull-out. In this case, the fibre strength is limited by the filler-polymer interfacial interaction.

For all fibres, the diameter, *D*, was measured at 10 positions along the fibre length using a profilometer (Dektak 6 M Stylus Profiler). In addition, the filler mass fraction was measured by thermogravimetric analysis (see SI). This was then converted to volume fraction, V_f, using the following density values ρ_G = 2200 kg/m^3, ρ_{BN} = 2370 kg/m^3 and ρ_{PVA} = 1300 kg/m^3. In Figure 2G and H it can be seen that both diameter and volume fraction scale with the ratio of the injection rate of the surfactant stabilized dispersion (ink) to the flow rate of the polymer in the glass pipe, F_{Ink} / F_{Poly}. In both cases, well-defined power law relationships are observed: $D \propto (F_{Ink} / F_{Poly})^{0.66}$ and $V_f \propto (F_{Ink} / F_{Poly})^{0.5}$. This is in line with previous reports[31] for coagulation-spun PVA/SWNT fibres (although the exponents are not identical). These relationships allow us some measure of control of D and V_f over reasonably wide ranges (~20μm<D<~100μm) and (~10%<V_f<~80%). However, it makes it very different to control the diameter and volume fraction independently, a fact that makes analysis problematic because fibre mechanical properties depend sensitively on both D and V_f.[31, 32] We note that these volume fractions are extremely high for nanocomposites. Usually, graphene-filled nanocomposites are limited to filler contents of a few vol% due to aggregation effects at higher loading levels.[11]

By comparison with polymer-nanotube composite fibres, it is likely that fibre spinning results in some flow-induced alignment of the nanosheets.[32, 83] This is supported by SEM images such as figure 2F, in which the protruding nanosheets appear to be somewhat aligned. Such alignment would be required to achieve the high volume fractions described here without large scale aggregation. In fact, rheological studies on solvent-dispersions of graphene nanosheets similar to those used here show nanosheet alignment to occur at volume fractions of ~0.15vol%.[84] Thus, it is likely that some level of nanosheet alignment occurs for all fibres produced in this study. In fact, we believe that this flow induced alignment is critical to the avoidance of large scale aggregation during spinning. We believe that aligned nanosheets can assemble together (separated by polymer) during the coagulation process in a relatively uniform and ordered way without the formation of nanosheet clumps separated by large polymer domains. We suggest this process is feasible (see below) as long as there is enough polymer to provide effective separation of the nanosheets. This is a critical difference between

coagulation spinning and bulk composite formation and allows a reasonable degree of dispersion to be achieved up to concentrations of 20 *vol%*.

3.2 Mechanical Properties of Fibres

We measured the tensile mechanical properties of the composite fibres for a range of filler loading levels, V_f. As mentioned above, because V_f was controlled via F_{Ink} / F_{Poly}, the fibre diameter varied significantly with graphene content. Representative stress–strain curves for the graphene- and BN-filled composites are shown in Figure 3A and 3B respectively. These stress strain curves are similar in shape to those reported for well dried coagulation spun PVA-nanotube composites.[32] However, they differ in one important point: both graphene- and BN-filled composites fail at strains of typically <2%, much lower than is usually found for coagulation spun PVA-based fibres[30-33, 43] (failure strains approaching 1000% have been observed in coagulation-spun nanotube-PVA fibres[43]). Low strain at break is usually observed when all solvent (which can act as a plasticising agent) is removed on drying.[32] However, it is not clear whether the observed brittleness is solvent related or due to the effects of the 2-dimensional fillers or their impact on polymer morphology.

We have extracted the Young's moduli, Y, and tensile strengths, σ_B, from the stress-strain curves, with this data plotted versus V_f in Fig 2C and 2B. For both composite types the strength and stiffness values appear to increase with volume fraction up to V_f~20% before falling off at higher loading levels. Such fall-offs at high loading level are quite common in nanocomposites and are generally assumed to be due to aggregation effects.[19, 85] We note that some aggregation of the nanosheets exists in the spinning dispersion due to the very high filler concentrations used. It is very unusual that the mechanical properties would keep increasing up to volume fractions as high as 20%. Usually, the peak reinforcement occurs at <1vol%.[10, 14] This implies that large scale aggregation is somehow suppressed by the fibre formation process, perhaps due to alignment effects as suggested above, with large scale aggregation occurring during coagulation only once V_f>20 *vol%*.

We believe that this aggregation suppression is due to a combination of nanosheet alignment and the large nanosheet thickness associated with the high concentration inks required for coagulation spinning. Assuming the nanosheets to be aligned, and taking a typical nanosheet thickness to be ~4.5 nm (~13 layers, see above), than at V_f=20% the mean spacing between nanosheets is ~18 nm. For the PVA molecular weight used here, the chain radius of

gyration is ~6 nm. This means that no more than 3 polymer molecules can fit between two adjacent nanosheets at this V_f. Thus, we suggest that at V_f=20% the inter-nanosheet spacing is close to the minimum spacing which can exist before aggregation occurs.

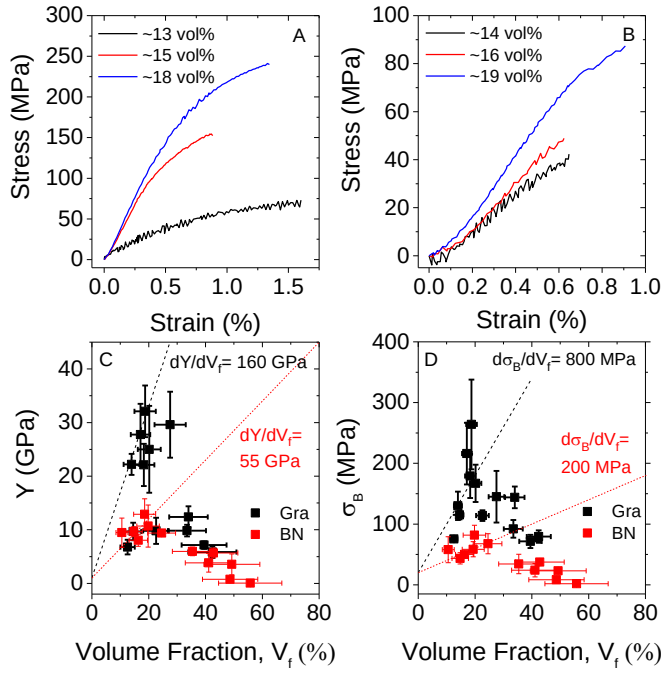

Figure 3. Representative stress strain curves of (A) Graphene- and (B) Boron Nitride-filled composites. (C) Ultimate Tensile Strength and (D) Young's Modulus of the composite fibres as a function of volume fraction. Dashed lines in (C) and (D) represent linear behaviour with slopes of dY/dV_f = 160 (black) and 55 (red) GPa and $d\sigma_B/dV_f$ = 800 (black) and 200 (red) MPa.

The peak values for modulus and all values for strength are considerably higher for graphene-filled composites compared to those incorporating BN. Peak values for modulus and strength for each composite were ~32 GPa and ~260 MPa respectively at V_f ~19 vol% for graphene-filled systems and ~13 GPa and ~82 MPa respectively at V_f = ~20 vol% for BN-filled materials. We note that these stiffness values are relatively high for graphene-containing fibres (see Figure 4). However, we note that these composite fibres have strengths which are considerably lower than the best fibres in the literature.

Because of the systematic variation of fibre diameter with volume fraction, it is difficult to apply any quantitative analysis to the mechanical properties of these fibres. Normally, the effectiveness of the reinforcing fillers can be assessed by the rate of increase of stiffness and strength with volume fraction at low loading levels (i.e. $d\sigma_B/dV_f$ and dY/dV_f). These

reinforcement metrics are normally related to intrinsic material properties via the rules of mixtures as given in equations 1 and 2. However, these equations cannot be applied directly because the fibre diameter is not constant and for real systems, both $d\sigma_B/dV_f$ and dY/dV_f are known to scale with diameter due to orientation and defect-related effects.[31] However, as shown by the dashed line in figure 3C all composites clearly have $dY/dV_f<160$ GPa (this line essentially plots equation 1 taking $Y_P=1$ GPa and $dY/dV_f=160$ GPa and applies to the graphene composites – for BN composites $dY/dV_f=55$ GPa). This is smaller than values recently reported for bulk composites of graphene in PVA (680 GPa)[10] or BN in PVA (670 GPa)[14] and well below the maximum value of 1000 GPa which is limited by the stiffness of graphene itself.[6] This lower-than-expected modulus reinforcement is in spite of the fact that the nanosheets are somewhat aligned and is partly due to the fact that the nanosheet aspect ratio is finite, resulting in $\eta_L<1$ (ref [8, 10]).

However, a more important factor may be nanosheet aggregation effects. We note that approximately one third of the 2D objects in the fibre spinning dispersion are aggregates. While such objects may provide some reinforcement to the fibre, their aggregated structure will mean that their contribution to the fibre strength and stiffness will be far lower than would be provided by individual nanosheets. In addition, even the individual nanosheets are few-layer, rather than monolayer with relatively large thicknesses due to high concentrations required to produce working inks. It is known that the effective nanosheet modulus tends to fall with nanosheet thickness.[15] Such effects could significantly suppress dY/dV_f compared to composites produced from thinner, less aggregated nanosheets.

As both graphene and BN are 2D filler materials with similar structure and mechanical properties[73] one would expect the mechanical performance of the two composite types to be similar. However this is not the case, with graphene-filled fibres displaying ~3 times better modulus and ~4 times better strength enhancement. The most obvious difference between fillers is the flake length (figure 1) with graphene flakes being approximately twice as large as BN flakes. However, both modulus and strength enhancement depend on aspect ratio (length/thickness) rather than length alone.[10] Thus for size effects to explain the performance differences, the graphene nanosheets would have to be not only longer than the BN ones but probably thinner as well. While this may be the case, we cannot effectively test it due to difficulties in accurately measuring thickness of liquid exfoliated nanosheets, especially aggregated ones.[70] An alternative explanation is suggested by the fact that the low volume fraction strength data displays lower slope ($d\sigma_B/dV_f$ ~200 MPa) for the BN-filled composites

compared to the graphene-filled systems ($d\sigma_B/dV_f$ ~800 MPa). Because this slope scales with the interfacial strength,[10] this implies the PVA-graphene interface to be roughly four times stronger than the PVA-BN interface. However, this is inconsistent with previous measurements on solution processed bulk PVA-graphene[10] and PVA-BN[14] composites where values of $d\sigma_B/dV_f$ =22 GPa and 47 GPa respectively were observed respectively. Alternatively, the difference may be associated with fibre formation: during spinning the BN dispersion was seen to coagulate in and around the injection syringe when coming in contact with the polymer solution. While this could possibly lead to poorer orientation or greater aggregation, such effects were not evident in the fibre morphology observed via SEM.

We note that fibre spinning can often result in alignment of the polymer chains themselves. Indeed, the fibre mechanical properties are very sensitive to the degree of chain alignment.[83] However, we feel this is unlikely to be the case here. While the relatively large (~µm) nanosheets can be relatively easily aligned due to the flow field in the pipe, alignment of the polymer chains would be much more challenging. In solution, the majority of chains exist as random coils with radius of gyration of ~5-6 nm. Orientation of such coils would incur a large entropic cost and be extremely unlikely at the low shear rates used in this work (assuming Poiseuille flow, the maximum shear rate in pipe was estimated to be ~30 s^{-1}). In any case, because the axial moduli and strength of aligned polymer chains are typically hundreds and tens of GPa respectively,[83] any significant alignment of the chains would be expected to result in levels of reinforcement far beyond those observed here.

In any case, the rates of increase of both modulus and strength with graphene volume fraction are considerably lower in these coagulation-spun fibres compared to bulk composites. However, this is more than compensated by the fact that the higher loading levels achievable here lead to much larger absolute stiffnesses and strengths. This makes the mechanical properties of these fibres competitive with other graphene (and nanotube) reinforced fibres (figure 4).

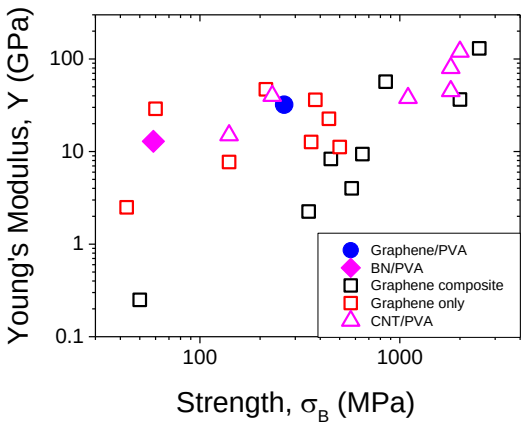

Figure 4: Comparison of best data reported here (filled symbols) to data for graphene and nanotube based fibres taken from the literature (see SI for table). The graphene literature data consists of graphene-oxide-only fibers and graphene-oxide composite fibers.

3.3 Electrical properties of Fibres

Because graphene is a conductor of electricity and, due to the very high loading levels in these fibres, we would expect them to display reasonably large electrical conductivities. We measured the conductivities of a number of fibres with the results shown in figure 5. We found the conductivity to increase with increasing graphene loading level, reaching 3 S/m for the 40 vol% sample. This value is higher than the maximum conductivity observed in most papers describing graphene-filled composites which tend to fall in the range 10^{-2}-10 S/m [refs[86-94]], although at least one paper described conductivities as high as 300 S/m.[95] In addition, this is considerably higher than the best results reported for most nanotube-filled composites.[96] For the lowest volume fractions, the conductivity was unmeasurably low.

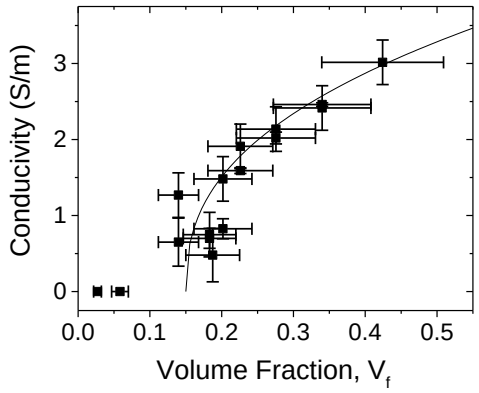

Figure 5. Electrical properties of PVA/graphene composite fibres. Conductivity of fibres plotted as a function of volume fraction. The dash line represents a fit to percolation theory and is consistent with $V_{f,c}$=15%, σ_0=5 S/m and t=0.4.

The electrical properties of composites consisting of conductive fillers in an insulating matrix, can be described by percolation theory.[97] In such systems, current can only flow once the conductor loading level is above a critical volume fraction known as the percolation threshold, $V_{f,c}$, where the first continuous conducting path across the matrix is formed. For $V_f > V_{f,c}$, the conductivity of the system is described by the percolation scaling law:

$$\sigma = \sigma_0 (V_f - V_{f,c})^t \quad (3)$$

where σ_0 is a crude measure of the conductivity of a network of the conducting material alone[76] and t is the percolation exponent. We have fit this equation to the data finding a reasonable agreement for $V_{f,c}$=15 vol%, t = 0.4 and σ_0=5 S/m. This percolation threshold is relatively high compared to reported values for bulk graphene filled composites which can be as low as 0.1vol%[98].This is almost certainly due to the alignment of the nanosheets within the fibre. Composites of aligned graphene nanosheets have previously been seen to have percolation thresholds as high as 15%.[76] In addition, simulations on conducting rod containing composites show the percolation threshold to increase with rod orientation.[99] The percolation exponent observed here is rather small and well below the expected value of 2 for transport in 3D. It is not clear why this exponent should be so low. While very low percolation exponents have been observed for thin film networks of both nanotubes and graphene (as low as 0.5),[100] percolation exponents in polymer-nanotubes composites are almost always >1.[96]

4. Conclusions

In this work we have demonstrated coagulation spinning of composites fibres filled with nanosheets of both graphene and BN. These fibres display both modulus and strength which increase with increasing nanosheet content up to ~20vol%, considerably higher than is usually observed. While aggregation effects result in rates of increase of modulus and strength with nanosheet volume fraction which are far below what is theoretically possible, the maximum modulus and strength observed were high; ~30 GPa and 260 MPa respectively. In addition, we found the graphene-filled fibres to be electrically conductive, displaying conductivities as high as 3 S/m.

Acknowledgements

We acknowledge the ERC for support via the project SEMANTICS. We have also received support from the Science Foundation Ireland (SFI) funded centre AMBER (SFI/12/RC/2278**).** We would also like to acknowledge additional funding from the Graphene Flagship (No. 604391).

References

[1] Allen MJ, Tung VC, Kaner RB. Honeycomb carbon: a review of graphene. Chem Rev. 2010;110(1):132-45.
[2] Castro Neto AH, Guinea F, Peres NMR, Novoselov KS, Geim AK. The electronic properties of graphene. Rev Mod Phys. 2009;81(1):109-62.
[3] Frank IW, Tanenbaum DM, Zande AMvd, McEuen PL. Mechanical properties of suspended graphene sheets. Journal of Vacuum Science & Technology B. 2007;25(6):2558-61.
[4] Geim AK. Graphene: Status and Prospects. Science. 2009;324(5934):1530-4.
[5] Geim AK, Novoselov KS. The rise of graphene. Nat Mater. 2007;6(3):183-91.
[6] Lee C, Wei X, Kysar JW, Hone J. Measurement of the elastic properties and intrinsic strength of monolayer graphene. Science. 2008;321(5887):385-8.
[7] Harris B. Engineering Composite Materials: Maney Materials Science; 1999.
[8] Padawer GE, Beecher N. On the strength and stiffness of planar reinforced plastic resins. Polym Eng Sci. 1970;10(3):185-92.
[9] Rosenthal J. A model for determining fiber reinforcement efficiencies and fiber orientation in polymer composites. Polym Compos. 1992;13(6):462-6.
[10] May P, Khan U, O'Neill A, Coleman JN. Approaching the theoretical limit for reinforcing polymers with graphene. Journal of Materials Chemistry. 2012;22(4):1278-82.
[11] Young RJ, Kinloch IA, Gong L, Novoselov KS. The mechanics of graphene nanocomposites: A review. Composites Science and Technology. 2012;72(12):1459-76.
[12] Gong L, Kinloch IA, Young RJ, Riaz I, Jalil R, Novoselov KS. Interfacial Stress Transfer in a Graphene Monolayer Nanocomposite. Advanced Materials. 2010;22(24):2694-+.
[13] Jan R, May P, Bell AP, Habib A, Khan U, Coleman JN. Enhancing the mechanical properties of BN nanosheet-polymer composites by uniaxial drawing. Nanoscale. 2014;6(9):4889-95.
[14] Khan U, May P, O'Neill A, Bell AP, Boussac E, Martin A, et al. Polymer reinforcement using liquid-exfoliated boron nitride nanosheets. Nanoscale. 2013;5(2).
[15] Gong L, Young RJ, Kinloch IA, Riaz I, Jalil R, Novoselov KS. Optimizing the Reinforcement of Polymer-Based Nanocomposites by Graphene. ACS Nano. 2012;6(3):2086-95.
[16] Du J, Cheng H-M. The Fabrication, Properties, and Uses of Graphene/Polymer Composites. Macromol Chem Phys. 2012;213(10-11):1060-77.
[17] Sengupta R, Bhattacharya M, Bandyopadhyay S, Bhowmick AK. A review on the mechanical and electrical properties of graphite and modified graphite reinforced polymer composites. Progress in Polymer Science. 2011;36(5):638-70.
[18] Kim H, Abdala AA, Macosko CW. Graphene/Polymer Nanocomposites. Macromolecules. 2010;43(16):6515-30.
[19] Kuilla T, Bhadra S, Yao D, Kim NH, Bose S, Lee JH. Recent advances in graphene based polymer composites. Progress in Polymer Science. 2010;35(11):1350-75.
[20] Fornes TD, Baur JW, Sabba Y, Thomas EL. Morphology and properties of melt-spun polycarbonate fibers containing single- and multi-wall carbon nanotubes. Polymer. 2006;47(5):1704-14.

[21] Haggenmueller R, Gommans HH, Rinzler AG, Fischer JE, Winey KI. Aligned single-wall carbon nanotubes in composites by melt processing methods. Chemical Physics Letters. 2000;330(3–4):219-25.
[22] Kearns JC, Shambaugh RL. Polypropylene fibers reinforced with carbon nanotubes. J Appl Polym Sci. 2002;86(8):2079-84.
[23] Kumar S, Doshi H, Srinivasarao M, Park JO, Schiraldi DA. Fibers from polypropylene/nano carbon fiber composites. Polymer. 2002;43(5):1701-3.
[24] Sandler JKW, Pegel S, Cadek M, Gojny F, van Es M, Lohmar J, et al. A comparative study of melt spun polyamide-12 fibres reinforced with carbon nanotubes and nanofibres. Polymer. 2004;45(6):2001-15.
[25] Siochi EJ, Working DC, Park C, Lillehei PT, Rouse JH, Topping CC, et al. Melt processing of SWCNT-polyimide nanocomposite fibers. Composites Part B: Engineering. 2004;35(5):439-46.
[26] Zeng J, Saltysiak B, Johnson WS, Schiraldi DA, Kumar S. Processing and properties of poly(methyl methacrylate)/carbon nano fiber composites. Composites Part B: Engineering. 2004;35(2):173-8.
[27] Behabtu N, Green MJ, Pasquali M. Carbon nanotube-based neat fibers. Nano Today. 2008;3(5–6):24-34.
[28] Ericson LM, Fan H, Peng H, Davis VA, Zhou W, Sulpizio J, et al. Macroscopic, Neat, Single-Walled Carbon Nanotube Fibers. Science. 2004;305(5689):1447-50.
[29] Valiavalappil S, Harinipriya S. Electrically conducting nylon 6,6–polyaniline short composite fibres synthesised by the solvent coagulation method. Synthetic Metals. 2012;162(23):2027-32.
[30] Vigolo B, Pénicaud A, Coulon C, Sauder C, Pailler R, Journet C, et al. Macroscopic Fibers and Ribbons of Oriented Carbon Nanotubes. Science. 2000;290(5495):1331-4.
[31] Young K, Blighe FM, Vilatela JJ, Windle AH, Kinloch IA, Deng L, et al. Strong Dependence of Mechanical Properties on Fiber Diameter for Polymer-Nanotube Composite Fibers: Differentiating Defect from Orientation Effects. ACS Nano. 2010;4(11):6989-97.
[32] Blighe FM, Young K, Vilatela JJ, Windle AH, Kinloch IA, Deng L, et al. The Effect of Nanotube Content and Orientation on the Mechanical Properties of Polymer-Nanotube Composite Fibers: Separating Intrinsic Reinforcement from Orientational Effects. Advanced Functional Materials. 2011;21(2):364-71.
[33] Dalton AB, Collins S, Munoz E, Razal JM, Ebron VH, Ferraris JP, et al. Super-tough carbon-nanotube fibres. Nature. 2003;423(6941).
[34] Chronakis IS. Novel nanocomposites and nanoceramics based on polymer nanofibers using electrospinning process—A review. Journal of Materials Processing Technology. 2005;167(2–3):283-93.
[35] Dror Y, Salalha W, Khalfin RL, Cohen Y, Yarin AL, Zussman E. Carbon Nanotubes Embedded in Oriented Polymer Nanofibers by Electrospinning. Langmuir. 2003;19(17):7012-20.
[36] Hou H, Ge JJ, Zeng J, Li Q, Reneker DH, Greiner A, et al. Electrospun Polyacrylonitrile Nanofibers Containing a High Concentration of Well-Aligned Multiwall Carbon Nanotubes. Chem Mater. 2005;17(5):967-73.
[37] Kim GM, Michler GH, Pötschke P. Deformation processes of ultrahigh porous multiwalled carbon nanotubes/polycarbonate composite fibers prepared by electrospinning. Polymer. 2005;46(18):7346-51.
[38] Ko F, Gogotsi Y, Ali A, Naguib N, Ye H, Yang Gl, et al. Electrospinning of Continuous Carbon Nanotube-Filled Nanofiber Yarns. Advanced Materials. 2003;15(14):1161-5.
[39] Li D, Wang Y, Xia Y. Electrospinning of Polymeric and Ceramic Nanofibers as Uniaxially Aligned Arrays. Nano Letters. 2003;3(8):1167-71.
[40] Salalha W, Dror Y, Khalfin RL, Cohen Y, Yarin AL, Zussman E. Single-Walled Carbon Nanotubes Embedded in Oriented Polymeric Nanofibers by Electrospinning. Langmuir. 2004;20(22):9852-5.
[41] Sen R, Zhao B, Perea D, Itkis ME, Hu H, Love J, et al. Preparation of Single-Walled Carbon Nanotube Reinforced Polystyrene and Polyurethane Nanofibers and Membranes by Electrospinning. Nano Letters. 2004;4(3):459-64.
[42] Ye H, Lam H, Titchenal N, Gogotsi Y, Ko F. Reinforcement and rupture behavior of carbon nanotubes–polymer nanofibers. Applied Physics Letters. 2004;85(10):1775-7.

[43] Miaudet P, Badaire S, Maugey M, Derre A, Pichot V, Launois P, et al. Hot-drawing of single and multiwall carbon nanotube fibers for high toughness and alignment. Nano Letters. 2005;5(11):2212-5.
[44] Dong J, Yin C, Zhao X, Li Y, Zhang Q. High strength polyimide fibers with functionalized graphene. Polymer. 2013;54(23):6415-24.
[45] He Y, Zhang N, Gong Q, Qiu H, Wang W, Liu Y, et al. Alginate/graphene oxide fibers with enhanced mechanical strength prepared by wet spinning. Carbohydrate Polymers. 2012;88(3):1100-8.
[46] Hou W, Tang B, Lu L, Sun J, Wang J, Qin C, et al. Preparation and physico-mechanical properties of amine-functionalized graphene/polyamide 6 nanocomposite fiber as a high performance material. Rsc Advances. 2014;4(10):4848-55.
[47] Jiang Z, Li Q, Chen M, Li J, Li J, Huang Y, et al. Mechanical reinforcement fibers produced by gel-spinning of poly-acrylic acid (PAA) and graphene oxide (GO) composites. Nanoscale. 2013;5(14):6265-9.
[48] Li J, Shao L, Zhou X, Wang Y. Fabrication of high strength PVA/rGO composite fibers by gel spinning. Rsc Advances. 2014;4(82):43612-8.
[49] Li Y, Sun J, Du Q, Zhang L, Yang X, Wu S, et al. Mechanical and dye adsorption properties of graphene oxide/chitosan composite fibers prepared by wet spinning. Carbohydrate Polymers. 2014;102:755-61.
[50] Navarro-Pardo F, Martinez-Barrera G, Laura Martinez-Hernandez A, Castano VM, Luis Rivera-Armenta J, Medellin-Rodriguez F, et al. Effects on the Thermo-Mechanical and Crystallinity Properties of Nylon 6,6 Electrospun Fibres Reinforced with One Dimensional (1D) and Two Dimensional (2D) Carbon. Materials. 2013;6(8):3494-513.
[51] Seyedin MZ, Razal JM, Innis PC, Jalili R, Wallace GG. Achieving Outstanding Mechanical Performance in Reinforced Elastomeric Composite Fibers Using Large Sheets of Graphene Oxide. Advanced Functional Materials. 2015;25(1):94-104.
[52] Tian M, Qu L, Zhang X, Zhang K, Zhu S, Guo X, et al. Enhanced mechanical and thermal properties of regenerated cellulose/graphene composite fibers. Carbohydrate Polymers. 2014;111:456-62.
[53] Liu Z, Xu Z, Hu X, Gao C. Lyotropic Liquid Crystal of Polyacrylonitrile-Grafted Graphene Oxide and Its Assembled Continuous Strong Nacre-Mimetic Fibers. Macromolecules. 2013;46(17):6931-41.
[54] Xu Z, Liu Z, Sun H, Gao C. Highly Electrically Conductive Ag-Doped Graphene Fibers as Stretchable Conductors. Advanced Materials. 2013;25(23):3249-53.
[55] Aboutalebi SH, Jalili R, Esrafilzadeh D, Salari M, Gholamvand Z, Aminorroaya Yamini S, et al. High-Performance Multifunctional Graphene Yarns: Toward Wearable All-Carbon Energy Storage Textiles. ACS Nano. 2014;8(3):2456-66.
[56] Xiang C, Young CC, Wang X, Yan Z, Hwang C-C, Cerioti G, et al. Large Flake Graphene Oxide Fibers with Unconventional 100% Knot Efficiency and Highly Aligned Small Flake Graphene Oxide Fibers. Adv Mater. 2013;25(33):4592-7.
[57] Zhao Y, Jiang C, Hu C, Dong Z, Xue J, Meng Y, et al. Large-Scale Spinning Assembly of Neat, Morphology-Defined, Graphene-Based Hollow Fibers. ACS Nano. 2013;7(3):2406-12.
[58] Chen L, He Y, Chai S, Qiang H, Chen F, Fu Q. Toward high performance graphene fibers. Nanoscale. 2013;5(13):5809-15.
[59] Xu Z, Sun H, Zhao X, Gao C. Ultrastrong Fibers Assembled from Giant Graphene Oxide Sheets. Advanced Materials. 2013;25(2):188-93.
[60] Cong H-P, Ren X-C, Wang P, Yu S-H. Wet-spinning assembly of continuous, neat, and macroscopic graphene fibers. Sci Rep. 2012;2.
[61] Dong Z, Jiang C, Cheng H, Zhao Y, Shi G, Jiang L, et al. Facile Fabrication of Light, Flexible and Multifunctional Graphene Fibers. Advanced Materials. 2012;24(14):1856-61.
[62] Jalili R, Aboutalebi SH, Esrafilzadeh D, Shepherd RL, Chen J, Aminorroaya-Yamini S, et al. Scalable One-Step Wet-Spinning of Graphene Fibers and Yarns from Liquid Crystalline Dispersions of Graphene Oxide: Towards Multifunctional Textiles. Advanced Functional Materials. 2013;23(43):5345-54.

[63] Shin MK, Lee B, Kim SH, Lee JA, Spinks GM, Gambhir S, et al. Synergistic toughening of composite fibres by self-alignment of reduced graphene oxide and carbon nanotubes. Nat Commun. 2012;3.
[64] Xiang C, Behabtu N, Liu Y, Chae HG, Young CC, Genorio B, et al. Graphene Nanoribbons as an Advanced Precursor for Making Carbon Fiber. ACS Nano. 2013;7(2):1628-37.
[65] Xu Z, Gao C. Graphene chiral liquid crystals and macroscopic assembled fibres. Nat Commun. 2011;2.
[66] Gomez-Navarro C, Burghard M, Kern K. Elastic properties of chemically derived single graphene sheets. Nano Letters. 2008;8(7):2045-9.
[67] Hernandez Y, Nicolosi V, Lotya M, Blighe FM, Sun Z, De S, et al. High-yield production of graphene by liquid-phase exfoliation of graphite. Nat Nanotechnol. 2008;3(9):563-8.
[68] Lotya M, Hernandez Y, King PJ, Smith RJ, Nicolosi V, Karlsson LS, et al. Liquid Phase Production of Graphene by Exfoliation of Graphite in Surfactant/Water Solutions. J Am Chem Soc. 2009;131(10):3611-20.
[69] Lotya M, King PJ, Khan U, De S, Coleman JN. High-Concentration, Surfactant-Stabilized Graphene Dispersions. ACS Nano. 2010;4(6):3155-62.
[70] Paton KR, Varrla E, Backes C, Smith RJ, Khan U, O'Neill A, et al. Scalable production of large quantities of defect-free few-layer graphene by shear exfoliation in liquids. Nat Mater. 2014;13(6):624-30.
[71] Varrla E, Paton KR, Backes C, Harvey A, Smith RJ, McCauley J, et al. Turbulence-assisted shear exfoliation of graphene using household detergent and a kitchen blender. Nanoscale. 2014;6(20):11810-9.
[72] Khan U, Young K, O'Neill A, Coleman JN. High strength composite fibres from polyester filled with nanotubes and graphene. Journal of Materials Chemistry. 2012;22(25).
[73] Duclaux L, Nysten B, Issi JP, Moore AW. Structure and low-temperature thermal conductivity of pyrolytic boron nitride. Phys Rev B. 1992;46(6):3362-7.
[74] Coleman JN, Lotya M, O'Neill A, Bergin SD, King PJ, Khan U, et al. Two-Dimensional Nanosheets Produced by Liquid Exfoliation of Layered Materials. Science. 2011;331(6017):568-71.
[75] Khan U, Porwal H, O'Neill A, Nawaz K, May P, Coleman JN. Solvent-Exfoliated Graphene at Extremely High Concentration. Langmuir. 2011;27(15):9077-82.
[76] Cunningham G, Lotya M, McEvoy N, Duesberg GS, Schoot Pvd, Coleman JN. Percolation scaling in composites of exfoliated MoS2 filled with nanotubes and graphene. Nanoscale. 2012;4(20):6260-4.
[77] Boland CS, Khan U, Backes C, O'Neill A, McCauley J, Duane S, et al. Sensitive, High-Strain, High-Rate Bodily Motion Sensors Based on Graphene-Rubber Composites. ACS Nano. 2014;8(9):8819-30.
[78] Khan U, May P, O'Neill A, Coleman JN. Development of stiff, strong, yet tough composites by the addition of solvent exfoliated graphene to polyurethane. Carbon. 2010;48(14):4035-41.
[79] Yao L, Haas TW, Guiseppi-Elie A, Bowlin GL, Simpson DG, Wnek GE. Electrospinning and Stabilization of Fully Hydrolyzed Poly(Vinyl Alcohol) Fibers. Chem Mater. 2003;15(9):1860-4.
[80] Li X, Zhao T, Wang K, Yang Y, Wei J, Kang F, et al. Directly Drawing Self-Assembled, Porous, and Monolithic Graphene Fiber from Chemical Vapor Deposition Grown Graphene Film and Its Electrochemical Properties. Langmuir. 2011;27(19):12164-71.
[81] Yang Z, Sun H, Chen T, Qiu L, Luo Y, Peng H. Photovoltaic Wire Derived from a Graphene Composite Fiber Achieving an 8.45 % Energy Conversion Efficiency. Angew Chem. 2013;125(29):7693-6.
[82] Hull D, Clyne TW. An Introduction to Composite Materials | Materials science. Cambridge University Press 1996 2015/02/04/15:40:22 [cited; Available from:
[83] Song K, Zhang Y, Meng J, Green EC, Tajaddod N, Li H, et al. Structural Polymer-Based Carbon Nanotube Composite Fibers: Understanding the Processing-Structure-Performance Relationship. Materials. 2013;6(6):2543-77.
[84] Barwich S, Coleman JN, Moebius ME. Yielding and flow of highly concentrated, few-layer graphene suspensions. Soft Matter. 2015;11(16):3159-64.
[85] Coleman JN, Khan U, Blau WJ, Gun'ko YK. Small but strong: A review of the mechanical properties of carbon nanotube–polymer composites. Carbon. 2006;44(9):1624-52.

[86] Li M, Gao C, Hu H, Zhao Z. Electrical conductivity of thermally reduced graphene oxide/polymer composites with a segregated structure. Carbon. 2013;65:371-3.
[87] Meng Q, Jin J, Wang R, Kuan H-C, Ma J, Kawashima N, et al. Processable 3-nm thick graphene platelets of high electrical conductivity and their epoxy composites. Nanotechnology. 2014;25(12).
[88] Qi X-Y, Yan D, Jiang Z, Cao Y-K, Yu Z-Z, Yavari F, et al. Enhanced Electrical Conductivity in Polystyrene Nanocomposites at Ultra-Low Graphene Content. Acs Applied Materials & Interfaces. 2011;3(8):3130-3.
[89] Yan D, Zhang H-B, Jia Y, Hu J, Qi X-Y, Zhang Z, et al. Improved Electrical Conductivity of Polyamide 12/Graphene Nanocomposites with Maleated Polyethylene-Octene Rubber Prepared by Melt Compounding. Acs Applied Materials & Interfaces. 2012;4(9):4740-5.
[90] Yang L, Zhang S, Chen Z, Guo Y, Luan J, Geng Z, et al. Design and preparation of graphene/poly(ether ether ketone) composites with excellent electrical conductivity. Journal of Materials Science. 2014;49(5):2372-82.
[91] Ye W, Zhang L, Li C. Facile fabrication of silica-polymer-graphene collaborative nanostructure-based hybrid materials with high conductivity and robust mechanical performance. Rsc Advances. 2015;5(32):25450-6.
[92] Yousefi N, Gudarzi MM, Zheng Q, Aboutalebi SH, Sharif F, Kim J-K. Self-alignment and high electrical conductivity of ultralarge graphene oxide-polyurethane nanocomposites. Journal of Materials Chemistry. 2012;22(25):12709-17.
[93] Zheng D, Tang G, Zhang H-B, Yu Z-Z, Yavari F, Koratkar N, et al. In situ thermal reduction of graphene oxide for high electrical conductivity and low percolation threshold in polyamide 6 nanocomposites. Composites Science and Technology. 2012;72(2):284-9.
[94] Zhou TN, Qi XD, Fu Q. The preparation of the poly(vinyl alcohol)/graphene nanocomposites with low percolation threshold and high electrical conductivity by using the large-area reduced graphene oxide sheets. Express Polymer Letters. 2013;7(9):747-55.
[95] Jia J, Sun X, Lin X, Shen X, Mai Y-W, Kim J-K. Exceptional Electrical Conductivity and Fracture Resistance of 3D Interconnected Graphene Foam/Epoxy Composites. ACS Nano. 2014;8(6):5774-83.
[96] Bauhofer W, Kovacs JZ. A review and analysis of electrical percolation in carbon nanotube polymer composites. Composites Science and Technology. 2009;69(10):1486-98.
[97] Stauffer D, Aharony A. Introduction To Percolation Theory: CRC Press; 1994.
[98] Stankovich S, Dikin DA, Dommett GHB, Kohlhaas KM, Zimney EJ, Stach EA, et al. Graphene-based composite materials. Nature. 2006;442(7100):282-6.
[99] White SI, DiDonna BA, Mu M, Lubensky TC, Winey KI. Simulations and electrical conductivity of percolated networks of finite rods with various degrees of axial alignment. Phys Rev B. 2009;79(2).
[100] De S, Coleman JN. The effects of percolation in nanostructured transparent conductors. MRS Bulletin. 2011;36(10):774-81.